

A Strongly Anisotropic Superconducting Gap in the Kagome Superconductor CsV_3Sb_5 : A Study of Directional Point-Contact Andreev Reflection Spectroscopy

Yu-qing Zhao^{1§}, Zhi-fan Wu^{1§}, Hai-yan Zuo¹, Weiming Lao¹, Wangju Yang¹, Qiuxia Chen¹, Yao He¹, Hai Wang¹, Qiangwei Yin², Qi Wang³, Yang-peng Qi³, Gang Mu⁴, He-chang Lei^{2†}, and Cong Ren^{1,5†}

¹ School of Physics and Astronomy, Yunnan University, Kunming 650500, China

² Department of Physics and Beijing Key Laboratory of Opto-electronic Functional Materials and Micro-nano Devices, Renmin University of China, Beijing 100872, China

³ School of Physical Science and Technology, ShanghaiTech University, Shanghai 201210, China

⁴ State Key Laboratory of Materials for Integrated Circuits, Shanghai Institute of Microsystem and Information Technology, Chinese Academy of Sciences, Shanghai 200050, China and

⁵ Yunnan Key Laboratory for Electromagnetic Materials and Devices, Yunnan University, Kunming 650500, China

In the recently discovered V-based kagome superconductors AV_3Sb_5 ($A = \text{K}, \text{Rb}, \text{and Cs}$), superconductivity is intertwined with an unconventional charge density wave (CDW) order, raising a fundamental concern on the superconducting gap structure of such kagome superconductor in the presence of CDW orders. Here, we report directional soft point-contact Andreev reflection (SPCAR) spectroscopy measurements on the kagome superconductor CsV_3Sb_5 , revealing compelling evidence for the existence of a strongly anisotropic superconducting gap pairing state. The SPCAR spectra measured with current injected parallel to the ab -plane exhibit an in-gap single conductance peak, in contrast to those of SPCAR spectra: a double-peak structure in the perpendicular direction. These spectra are well described by an anisotropic single-gap BTK model. The extracted superconducting gaps comprise an isotropic large gap and a strongly anisotropic gap, originating from different Fermi surface sheets. Quantitative analysis reveals an anisotropy around $\sim 70\%$ with a gap minimum of about 0.15 meV. These results shew new light on the unconventional multiband pairing states in kagome superconductors.

1. Introduction: Kagome lattices, characterized by their unique two-dimensional network of corner-sharing triangles, have long captivated the condensed matter physics community as fertile ground for exploring novel quantum phenomena, which arise from strong electron correlations and magnetic frustration inherent to the kagome geometry [1–6]. This paradigm shifted dramatically with the recent discovery of superconductivity in a new class of materials: the vanadium-based kagome superconductors (SCs) AV_3Sb_5 ($A = \text{K}, \text{Rb}, \text{Cs}$). These compounds realize an ideal, non-magnetic kagome net of vanadium atoms with superconducting critical temperatures $T_c \sim 1 - 3 \text{ K}$ [7–11]. More intriguingly, the emergence of superconductivity is intertwined with unconventional charge density wave (CDW) orders in these kagome metals [12–21]. Understanding the nature of this superconductivity and its interplay with the CDW orders within the unique kagome framework, potentially distinct from conventional mechanisms, is now a central focus in quantum materials research.

As a fundamental parameter clarifying the microscopic pairing mechanism and interplays between multiple electronic orders, the superconducting gap structure or order parameter in kagome superconductors remain highly controversial and no consensus has yet been reached. Indeed, the observations of the Hebel-Slichter coherent peak in the spin-lattice relaxation rate from the NMR studies of CsV_3Sb_5 indicated a nodeless s -wave superconductivity [22]. Magnetic penetration depth [23] along with specific heat [13] measurements collectively point

to two nodeless gaps in weak-coupling limit in CsV_3Sb_5 . Such two isotropic gaps but in strong coupling limit have been confirmed in point-contact Andreev reflection spectrum [24, 25]. On the contrary, thermal conductivity measurements in CsV_3Sb_5 and μSR measurements in $\text{K/RbV}_3\text{Sb}_5$ have suggested the presence of a nodal gap in such V-based kagome superconductors [26, 27]. While low- T scanning tunneling microscopy (STM) appeared to show both nodal and nodeless sign-preserving gaps with multiple Fermi surfaces for the same material [28, 29], the latest angle-resolved photoemission spectroscopy (ARPES) measurements of high-quality CsV_3Sb_5 single crystals revealed that the SC gap in the β Fermi surface is strongly anisotropic with anisotropy $\sim 80\%$, suggesting the possible presence of a node gap [30]. Moreover, it has been reported that the anisotropy in the SC gap of CsV_3Sb_5 can be suppressed by electron irradiation [31], leading to a nodal-nodeless gap structure transition, similar to the case of nodal s_{\pm} -wave SC $\text{BaFe}_2(\text{As}_{1-x}\text{P}_x)_2$ [32–34]. These studies with different conclusions reflect the complexity of the system, and the direct measurement of the SC gap structure in such kagome superconductor is highly desired.

Point-contact Andreev reflection (PCAR) spectroscopy, some extent equivalent to tunneling spectroscopy, is a well-established technique for probing gap structure of superconductor [35, 36]. Based on some sophisticated theoretical models, PCAR spectra have also been proven to be suitable to study unconventional superconductors with “exotic” properties such as

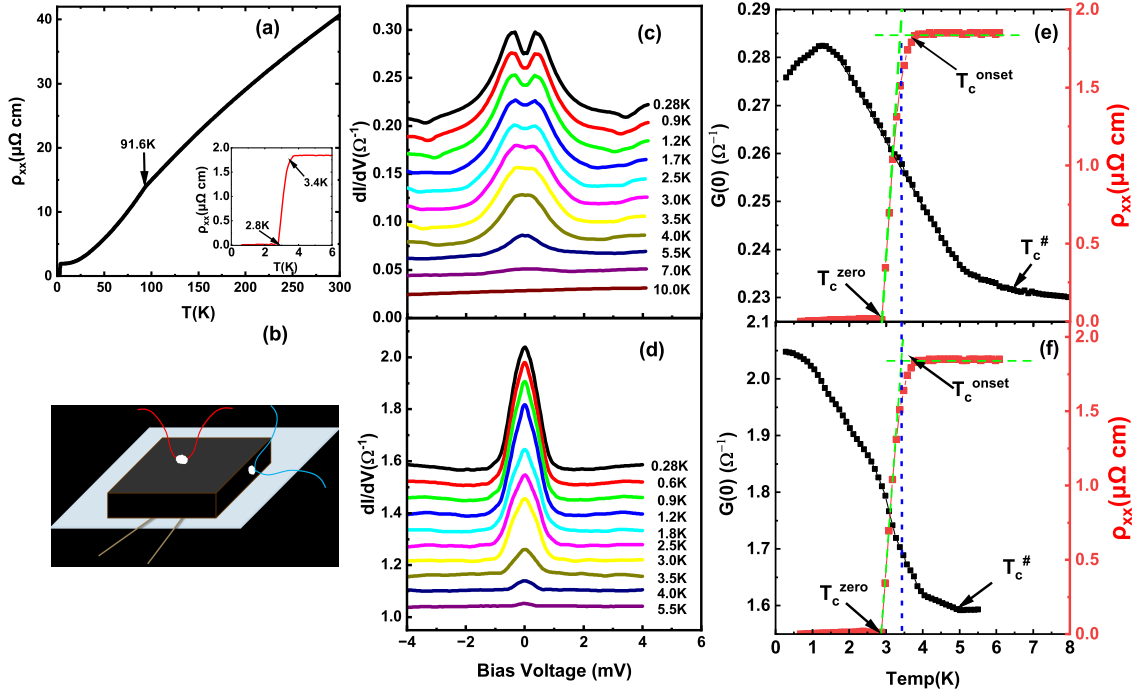


FIG. 1: (a) Temperature dependence of the in-plane resistivity ρ_{xx} of CsV₃Sb₅ single crystal, a pronounced kink at approximately 91.6 K indicates the onset of the charge density wave (CDW) transition. The inset magnifies the low-temperature region, showing the superconducting transition with the onset temperature T_c^{onset} and zero-resistivity temperature T_c^{zero} marked. (b) Schematic of the “soft” point-contact spectroscopy measurement configuration. The black block represents the CsV₃Sb₅ single crystal, while the red and blue lines indicate the injection paths for soft point-contact Andreev reflection measurements with current applied perpendicular (labeled as *c*-axis junction) and parallel (labeled as *ab*-plane junction) to the *ab*-plane, respectively. (c)(d) T -dependent point-contact conductance spectra $G \equiv dI/dV$ measured with sensing current I along *c*-axis (“*c*-axis” junction) (c) and along *ab*-plane (*ab*-plane junction), respectively. (e)(f) T -dependence of the zero-bias conductance $G(0)$ of CsV₃Sb₅/Ag point contacts for *c*-axis (e) and *ab*-plane junctions (f), respectively. The bulk resistivity ρ_{xx} in the superconducting transition region is presented for comparison.

anisotropic, nodal/nodeless, and multiple SC gaps. One advantage of PCAR spectroscopy in studying the superconducting gap structure is that point-contact junction can be flexibly fabricated on the surface of the superconducting crystals under study. In this study, we conduct a directional PCAR spectroscopy study on CsV₃Sb₅ to investigate its superconducting gap structure by fabricating *c*-axis and *ab*-plane point contacts on CsV₃Sb₅ single crystals. These conductance spectra clearly feature the presence of an anisotropic gap besides two isotropic gaps.

2. Experiment Details: Single crystals of CsV₃Sb₅ were synthesized using the self-flux method, in two different laboratories whose crystals are labeled as #1 and #2, respectively. Figure 1(a) displays the temperature T dependence of the in-plane resistivity, $\rho_{xx}(T)$, measured on a single crystal of CsV₃Sb₅. The crystal demonstrates a metallic characteristics, quantified by a residual resistivity ratio defined as $RRR \equiv R(300, \text{K})/R(5, \text{K}) = 22$. A resistivity anomaly around 92 K corresponds to a well-defined charge density wave (CDW) phase [13]. The inset of Fig. 1(a) further details the superconducting transition observed at low temperatures, identifying a super-

conducting onset temperature $T_c^{\text{onset}} \approx 3.4$ K and a zero-resistance temperature $T_c^{\text{zero}} \approx 2.8$ K.

Point-contact to the CsV₃Sb₅ crystals were formed by a so-called “soft” point-contact technique [37]. This method involves attaching a platinum wire with a diameter of 16 μm , coated with a 50–100 μm in size of silver paint, to the cleaved surface of a CsV₃Sb₅ single crystal with a typical crystal dimensions $2.5 \times 2.0 \times 0.3 - 0.5$ mm³ along the *a*, *b*, and *c* crystallographic axes, respectively. In this configuration, the heterocontact is actually composed of many nanocontacts due to the nanocrystalline nature of the silver paint, mimic to the tip point-contact technique. Schematic of point-contact junction in our experiment are shown in Figure 1(b). Two kind of point-contact were formed: the write point-contact on *ab* plane (labeled as “*c*-axis” junction) and the red-colored point-contact on *ac/bc* plane (labeled as “*ab*-plane” junction). For the *ab*-plane configuration, the crystal was cleaved perpendicular to the *ab*-plane and polished using 10,000-grit sandpaper to produce a flat surface (*ac/bc*-plane), onto which the platinum wire was then bonded with silver paint. The differential conductance spectra $G(V)$

were recorded with the standard phase-sensitive lock-in technique in a quasi-four-terminal configuration, where an ac modulation was applied to the sample on top of a DC current bias. The contact resistance R_J between the nanoparticle of silver paint and CsV_3Sb_5 crystals was usually in the range of $0.5 - 10 \Omega$, typical values of a genuine point contact between normal metals and superconductors.

3. Results and Discussions: Figures 1(c) and 1(d) present the typical T -dependent c -axis and ab -plane SP-CAR conductance spectra $G(V) \equiv dI/dV$ of CsV_3Sb_5 crystals, respectively. A striking feature in these two kind of $G(V)$ curves is that: at lowest $T=0.28$ K, a conductance double peak around gap edge plus a zero-bias conductance dip in c -axis junction, on the other hand, an in-gap conductance peak in $G(V)$ for ab -plane junction. Qualitatively, for highly transparent junctions at finite T s, the appearance of a double-peak structure at gap-edge in the Andreev conductance spectrum is a characteristic of a nodeless gap state. In contrast, an in-gap conductance peak is a signature of an anisotropic gap state due to the presence of a finite DOS at low energy, like a d -wave gap in cuprates. Another feature in these point-contact spectrum is the appearance of the excess conductance spectrum at $T > T_c$. For example, Fig. 1(c) depicts T -evolution of c -axis point-contact spectra, exhibiting a two-distinct coherent peaks at gap-edge. As T increases above $T_c \simeq 3.4$ K, significant residual Andreev conductance persists before completely disappearing above $T^\# \sim 6.5$ K. The same is true for ab -plane junctions shown in Fig. 1(d), that the ab -plane point-contact spectra vanish entirely at a temperature of $T^\# \sim 5.5$ K. Figures 1(e) and 1(f) compare the temperature dependence of zero-bias conductance $G(0)$ with the in-plane resistivity ρ_{xx} . These plots clearly demonstrate a persistent conductance “tail” up to $T_c^\#$. This phenomenon of excess conductance spectra has been consistently observed in prior soft point-contact studies on CsV_3Sb_5 and KV_3Sb_5 [24, 25]. We emphasize that six separate CsV_3Sb_5 samples were measured, yielding six distinct sets of Andreev reflection spectra, all of which exhibits nearly identical spectral behaviors.

To quantitatively assess the gap structure of CsV_3Sb_5 , we examined the PCAR spectroscopy along with the sensing current parallel to both the c -axis and ab -plane junctions for two different CsV_3Sb_5 samples (#1 and #2). Fig. 2(a) and 2(b) show the normalized Andreev conductance spectra $G(V)/G_N$ at the lowest T of 0.28 K with sensing current along the c -axis (c -axis junction) for #1 and #2, respectively. As shown, the c -axis junctions clearly show a double-peak features in PCAR spectra, signaling a nodeless gap state. Based on prior PCAR studies [24, 25], the spectra are more accurately described using a modified Blonder–Tinkham–Klapwijk (BTK) model with two s -wave conductance channels $G(V) = \omega G_S(V) + (1 - \omega)G_L(V)$, where ω quantifies the

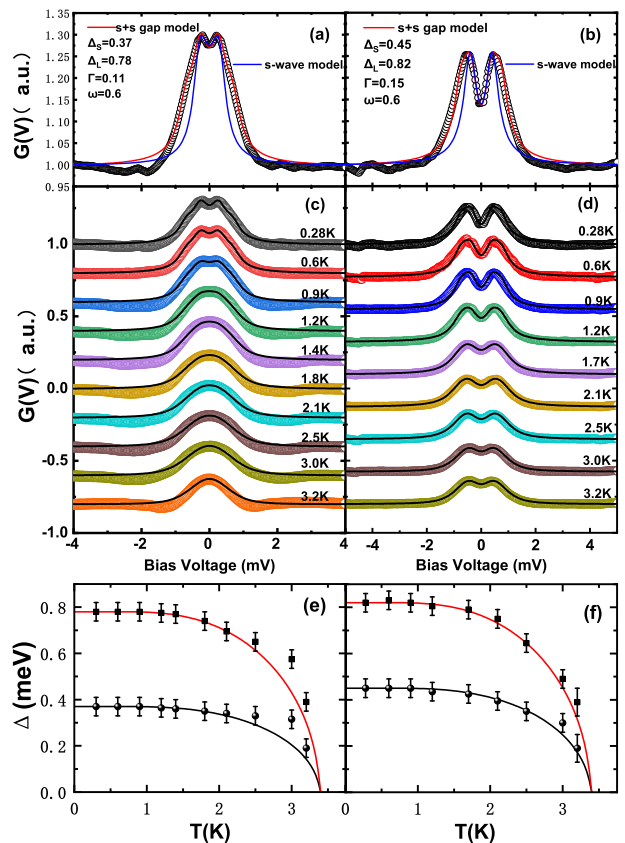


FIG. 2: (a)(b) The normalized c -axis Andreev conductance spectrum $G(V)/G_N$ at the lowest $T = 0.28$ K for #1 and #2 junctions, respectively. The solid red curves are their BTK fits with a two-isotropic gap model. The solid blue curves are their BTK fits with a single s -wave gap model, for comparison. (c)(d) The normalized c -axis Andreev conductance spectra $G(V)/G_N$ at various T s from 0.28 K to 3.5 K #1 (c) and #2 (d) junctions, respectively. The solid curves are their BTK fits using a two-isotropic gap model. (e)(f) The corresponding superconducting gap $\Delta(T)$ as a function of T , which closely follows the BCS $\Delta - T$ function.

relative spectral weight of the two channels. Noted we also analyzed such PCAR spectral data of c -axis junctions using a single s -wave gap model for comparison, as shown in Fig. 2(a) and 2(b). The two s -wave-gap fitting give the best result, yielding a small gap value of $\Delta_S \simeq 0.37$ meV for #1 and 0.45 meV for #2, and a large gap value of $\Delta_L \simeq 0.78$ meV (#1) and 0.82 meV (#2), with the spectral weight of $\omega \sim 0.60$ for both junctions. The corresponding broadening parameters Γ are $\Gamma_S \simeq 0.13$ meV (#1) and 0.15 meV (#2), respectively. The barrier strength, or junction transparency are $Z = 0.54$ and 0.78 for junction #1 and #2, respectively. Note that an isotropic two-gap model cannot produce reasonable results.

The T -dependent PCAR spectra and their fits based on the above-obtained parameters are shown in Fig. 3(c) and 3(d) for #1 and #2, respectively. As shown, the

two s -wave gap BTK model provides good fits to all $G(V)$ curves. In the fitting process, ω is kept constant for each sample, while Γ increases slightly with T up to T_c . The resulting gaps Δ_L and Δ_S for samples #1 and #2 are plotted as a function of T , shown in Figs. 2(e) and 2(f), respectively. The obtained gaps can be approximated by an empirical BCS formula: $\Delta(T) = \Delta_0 \tanh(\alpha\sqrt{T_c/T} - 1)$ where α is adjustable parameter. For samples #1 and #2, $\Delta_L \sim 0.80$ meV, and $\Delta_S \sim 0.41$ meV. Thus, the coupling strength is estimated as: $2\Delta_L/k_B T_c \simeq 5.47$ for larger superconducting gap in strong coupling limit, and $2\Delta_S/k_B T_c \simeq 2.73$ for smaller superconducting gap in weak-coupling strength, in align quantitatively with those values of the prototypical two-gap superconductor MgB₂ [37, 38], in which the superconducting gaps satisfy the relation $2\Delta_L/k_B T_c > 2\Delta_{\text{BCS}}/k_B T_c(3.52) \geq 2\Delta_S/k_B T_c$ [39]. These values are in good agreement with previously reported results on the similar CsV₃Sb₅ c -axis junctions [24, 25].

On the other aspect, the point-contact spectra with sensing current I along the ab -plane (ab -plane junction) shown in Figs. 3(a) and 3(b) display a single broad zero-bias conductance peak in the gap region, characteristic of an anisotropic gap. These spectra are fitted to an anisotropic s -wave BTK model. Considering the six-fold symmetry inherent to the Kagome lattice and insights from ARPES measurements, we model the anisotropic s -wave superconducting gap using the form $\Delta^a \times [(1-r) + r \cos^2(3\theta)]$ [40] or the equivalently $\Delta^a \times [(1-r) + r \cos(6\theta)]$ [31]. In this gap function, r represents the gap anisotropy ratio, varying from $r = 0$ (isotropic s -wave state) to $r = 1$ (completely nodal gap state). As shown, the anisotropic gap BTK model provides an excellent description of the normalized $G(V)$ at the lowest T . The fits yield $\Delta^a \simeq 0.50$ meV for #1 crystal and 0.49 meV for #2 crystal, and $\Gamma = 0.18$ meV for both junctions. The gap anisotropy ratio $r = 0.70 \pm 0.10$ is resolved for the anisotropic gap of the ab -plane junctions.

Figures 3(c) and 3(d) show the normalized point-contact conductance spectra of the ab -plane junction, measured over a temperature range from 0.28 K to 3.4 K. The experimental data were fitted to the anisotropic-gapped BTK model. In the fitting process, the anisotropy $r = 0.70$ keep constant. The temperature evolution of the anisotropic gap extracted from the fits is presented in Fig.3(e) and 3(f) for #1 and #2, respectively. The extracted SC gap Δ^a obeys the BCS gap- T formula with the anisotropic SC gap $\Delta^a \simeq 0.50$ meV in the superconducting ground state. Based on these obtained values, there exists a gap minimum $\Delta_{\text{mini}}^a = \Delta^a(1-r) \simeq 0.15$ meV. Recently, a prominent ARPES experiment directly measure the SC gap in the momentum space in CsV₃Sb₅ single crystals. It is shown that the SC gaps in the α -band Fermi surface which from Sb-5 p orbital and δ -band Fermi surface from V-3 d orbital are isotropic, whereas the SC gap in the β Fermi surface from induced V-3 d

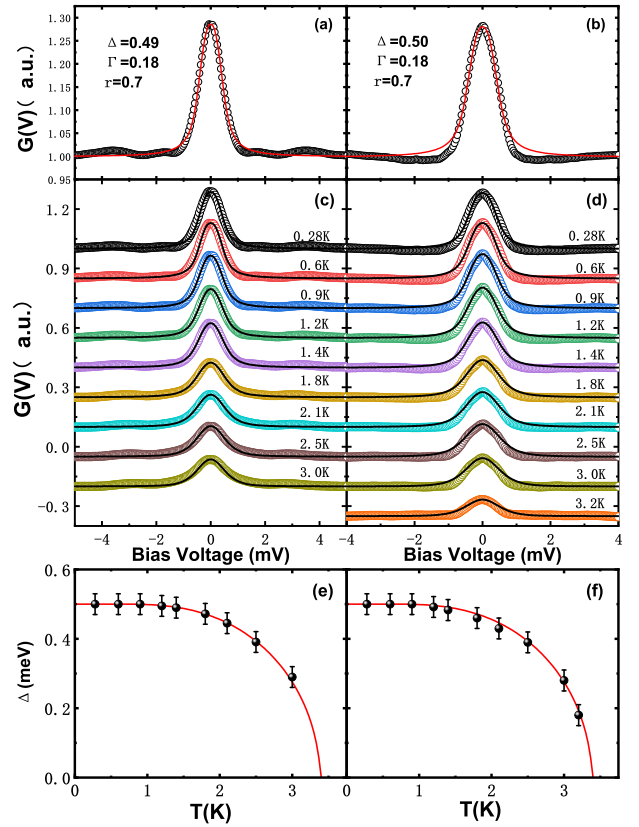


FIG. 3: (a)(b) The normalized ab -plane Andreev conductance spectrum $G(V)/G_N$ at the lowest $T = 0.28$ K for #1 and #2 junctions, respectively. The solid red curves are their BTK fits with an anisotropic gap model. (c)(d) The normalized ab -plane Andreev conductance spectra $G(V)/G_N$ at various T s from 0.28 K to 3.5 K #1 (c) and #2 (d) junctions, respectively. The solid curves are their BTK fits using an anisotropic gap model. All the conductance spectra and their corresponding fitting curves are shifted downward for clarity, excepted the top ones. (e)(f) The corresponding superconducting gap $\Delta(T)$ as a function of T , which closely follows the BCS $\Delta - T$ function.

orbital is highly anisotropic with a gap minimum of 0.10 meV [30]. Such a nodal s -wave gap, without sign reversal of SC order parameter, is completely consistent with our soft PCAR results.

In final, our Andreev reflection spectroscopy measurements reveal a significant gap anisotropy in CsV₃Sb₅, quantified at approximately 70% with a gap minimum 0.15 meV. However, given the known strong suppression of gap anisotropy by disorder/impurity effect in kagome superconductors, and the limited sample purity (indicated by the residual resistivity ratio, RRR), this measured value likely represents a lower bound. We posit that in intrinsically clean CsV₃Sb₅ samples, the gap anisotropy could approach 100%, implying possibly a true node gap.

4. *Conclusion:* A directional PCAR experiment was performed to probe the SC gap structure of kagome su-

perconductor CsV_3Sb_5 . The point-contact Andreev conductance spectra feature a strongly anisotropic gapping behavior, signalling the existence of an anisotropic gap in addition to isotropic SC gaps. Quantitative analysis of the spectral data estimates a gap-anisotropy $\sim 70\%$ and the gap minimum ~ 0.15 meV. Our direct observation of the orbital-selective anisotropic Cooper pairing in pristine CsV_3Sb_5 points to the unconventional pairing mechanisms and could also be consistent with the SC gap structure of a 2×2 pair density wave, providing a foundation for further understanding the intertwinement with other electronic ordering states, such as the time-reversal symmetry breaking, loop current ordering and electronic nematicity.

-
- [1] Norman M R, *Colloquium: Herbertsmithite and the search for the quantum spin liquid* 2016 Rev. Mod. Phys. 88 041002.
 - [2] Balents L, *Spin liquids in frustrated magnets* 2010 Nature 464 199.
 - [3] Liu Enke, Sun Yan, Kumar Nitesh, Muechler L, Sun A L, Jiao L, Yang S Y, Liu D F, Liang A J, Xu Q N, Kroder Johannes, Süß V, Borrmann H, Shekhar C, Wang Z S, Xi C Y, Wang W H, Schnelle W, Wirth S, Chen Y L, Goennenwein S T, and Felser C, *Giant anomalous Hall effect in a ferromagnetic kagome-lattice semimetal* 2015 Nat. Phys. 14 1125.
 - [4] Liu D F, Liang A J, Liu E K, Xu Q N, Li Y W, Chen C, Pei D, Shi W J, Mo S K, Dudin P, Kim T, Cacho C, Li G, Sun Y, Yang L X, Liu Z K, Parkin S S, Felser C, Chen Y L, *Magnetic Weyl semimetal phase in a Kagome crystal* 2019 Science 365 1282.
 - [5] Kiesel M L, Platt C, and Thomale R, *Unconventional Fermi surface instabilities in the Kagome Hubbard model* 2013 Phys. Rev. Lett. 110 126405.
 - [6] Wang W S, Li Z Z, Xiang Y Y, and Wang Q H, *Competing electronic orders on kagome lattices at van Hove filling* 2013 Phys. Rev. B 87 115135.
 - [7] Ko W H, Lee P A, and Wen X G, *Doped kagome system as exotic superconductor* 2009 Phys. Rev. B 79 214502
 - [8] Yu S L and Li J X, *Chiral superconducting phase and chiral spin-density-wave phase in a Hubbard model on the kagome lattice* 2012 Phys. Rev. B 85 144402
 - [9] Ortiz B R, Teicher S M L, Hu Y, Zuo J L, Sarte P M, Schueller E C, Abeykoon A M M, Krogstad M J, Rosenkranz S, Osborn R, Seshadri R, Balents L, He J, and Wilson S D, *CsV_3Sb_5 : A Z_2 Topological Kagome Metal with a Superconducting Ground State* 2020 Phys. Rev. Lett. 125 247002
 - [10] Yin Q W, Tu Z J, Gong C S, Fu Y, Yan S H, and Lei H C, *Superconductivity and Normal-State Properties of Kagome Metal RbV_3Sb_5 Single Crystals* 2021 Chin. Phys. Lett. 38 037403.
 - [11] Ortiz B R, Gomes L C, Morey J R, Winiarski M, Bordelon M, Mangum J S, Oswald I W H, Rodriguez-Rivera J A, Neilson J R, Wilson S D, Ertekin E, McQueen T M, and Toberer E S, *New kagome prototype materials: discovery of KV_3Sb_5 , RbV_3Sb_5 , and CsV_3Sb_5* 2019 Phys. Rev. Materials 3 094407.
 - [12] Ortiz B R, Sarte P M, Kenney E M, Graf M J, Teicher S M L, Seshadri R, Wilson S D, *Fermi surface mapping and the nature of charge-density-wave order in the kagome superconductor CsV_3Sb_5* 2021 Phys. Rev. Mater. 5 034801.
 - [13] Ortiz B R, Sarte Paul M, Kenney E M, Graf M J, Teicher S M L, Seshadri Ram, and Wilson S D, *Superconductivity in the Z_2 kagome metal KV_3Sb_5* 2021 Phys. Rev. Materials 5 034801.
 - [14] Jiang Yu-Xiao, Yin Jia-Xin, Denner M. Michael, Shumiyta Nana, Ortiz B R, Xu Gang, Guguchia Z, He Junyi, Hossain Md, Liu Xiaoxiong, Ruff Jacob, Kautzsch Linus, Zhang S T, Chang G Q, Belopolski Ilya, Zhang Qi, Cochran T A, Multer Daniel, Litskevich Maksim, Cheng Zi-Jia, Yang X P, Wang Z Q, Thomale Ronny, Neupert Titus, Wilson S D, Hasan M Z, *Discovery of unconventional chiral charge order in kagome superconductor KV_3Sb_5* 2021 Nature Materials 20 1353.
 - [15] Tan H X, Liu Y Z, Wang Z Q, and Yan B H, *Charge density waves and electronic properties of superconducting kagome metals* 2021 Phys. Rev. Lett. 127 046401.
 - [16] Nie L P, Sun K L, Ma W R, Song D W, Zhang L X, Liang Z W, Wu P, Yu F H, Li J, Shan M, Zhao D, Li S J, Kang B L, Wu Z M, Zhao Y B, Liu K, Xiang Z J, Ying J J, Wang Z Y, Wu T, and Chen X H, *Charge-density-wave-driven electronic nematicity in a kagome superconductor* 2022 Nature 604 59
 - [17] Wilson S D and Ortiz B R, *AV_3Sb_5 kagome superconductors* 2024 Nat. Rev. Mater. 9 420.
 - [18] Jiang Kun, Wu Tao, Yin Jia-Xin, Wang Zhenyu, Hasan M Y, Wilson Stephen D, Chen X H, and Hu J P, *Kagome superconductors AV_3Sb_5 ($A = \text{K}, \text{Rb}, \text{Cs}$)* 2023 National Science Review 10: nwac199.
 - [19] Song Boqin, Ying Tianping, Wu Xianxin, Xia Wei, Yin Qiangwei, Zhang Qinghua, Song Yanpeng, Yang Xiaofan, Guo Jiangang, Gu Lin, Chen Xiaolong, Hu Jiangping, Andreas Schnyder P, Lei Hechang, Guo Yanfeng, Li Shiyan, *Anomalous enhancement of charge densitywave in kagome superconductor CsV_3Sb_5 approaching the 2D limit* 2023 14 2492.
 - [20] Zheng Lixuan, Wu Zhimian, Yang Ye, Nie Linpeng, Shan Min, Sun Kuanglv, Song Dianwu, Yu Fanghang, Li Jian, Zhao Dan, Li Shunjiao, Kang Baolei, Zhou Yanbing, Liu Kai, Xiang Ziji, Ying Jianjun, Wang Zhenyu, Wu Tao, Chen Xianhui, *Emergent charge order in pressurized kagome superconductor CsV_3Sb_5* 2022 Nature 611 682.
 - [21] Asaba T, Onishi A, Kageyama Y, Kiyosue T, Ohtsuka K, Suetsugu S, Kohsaka Y, Gaggli T, Kasahara Y, Murayama H, Hashimoto K, Tazai R, Kontani H, Ortiz B R, Wilson S D, Li Q, Wen H H, Shibauchi T, and Matsuda Y, *Evidence for an odd-parity nematic phase above the charge-density-wave transition in a kagome metal* 2024 Nat. Phys. 20 40.
 - [22] Mu C, Yin Q, Tu Z, Gong C, Lei H, Li Z, and Luo J, *S-wave superconductivity in kagome metal CsV_3Sb_5 revealed by $^{121/123}\text{Sb}$ NQR and ^{51}V NMR measurements* 2021 Chin. Phys. Lett. 38 077402.
 - [23] Duan, W. et al. *Nodeless superconductivity in the kagome metal CsV_3Sb_5* 2021 Sci. China Phys. Mech. Astron. 64 1.
 - [24] Yin L C, Zhang D T, Chen C F, Ye G, Yu F H, Ortiz B R, Luo S S, Duan W Y, Su H, Ying J J, Wilson S D, Chen X H, Yuan H Q, Song Y, and Lu X, *Strain-*

- sensitive superconductivity in the kagome metals KV_3Sb_5 and CsV_3Sb_5 probed by point-contact spectroscopy* 2021 Phys. Rev. B 104 174507.
- [25] He M C, Zi H, Zhan H X, Zhao Y Q, Ren C, Hou X Y, Shan L, Wang Q H, Yin Q W, Tu Z, Gong C, Lei H, Lu Z Y, Wang Q, Qi Y P, Chen G F, and Xiong P, *Strong-coupling superconductivity in the kagome metal CsV_3Sb_5 revealed by soft point-contact spectroscopy* 2022 Phys. Rev. B 106 104510.
- [26] Zhao C C, Wang L S, Xia W, Yin Q W, Ni J M, Huang Y Y, Tu C P, Tao Z C, Tu Z J, Gong C S, Lei H C, Guo Y F, Yang X F, and Li S Y. *Nodal superconductivity and superconducting domes in the topological kagome metal CsV_3Sb_5* 2021 <https://doi.org/10.21203/rs.3.rs-404809/v1>.
- [27] Gupta R, Das D, Mielke C H III, Guguchia Z, Shiroka T, Baines Ch, Bartkowiak M, Luetkens H, Khasanov R, Yin Q W, Tu Z J, Gong C S and Lei H C, *Microscopic evidence for anisotropic multigap superconductivity in the CsV_3Sb_5 kagome superconductor* 2022 npj Quantum Materials 7 49.
- [28] Xu Han-Shu, Yan Ya-Jun, Yin Ruotong, Xia Wei, Fang Shijie, Chen Ziyuan, Li Yuanji, Yang Wenqi, Guo Yanfeng, Feng Dong-Lai, *Multiband superconductivity with sign-preserving order parameter in kagome superconductor CsV_3Sb_5* 2021 Phys. Rev. Lett. 127 187004 (2021).
- [29] Chen H, Yang H T, Hu B, Zhao Z, Yuan J, Xing Y Q, Qian G J, Huang Z H, Li G, Ye Y H, Ma S, Ni S L, Zhang H, Yin Q W, Gong C S, Tu Z J, Lei H C, Tan H X, Zhou S, Shen C M, Dong X L, Yan B H, Wang Z Q, and Gao H J, *Roton pair density wave in a strong-coupling kagome superconductor* 2021 Nature 599 222.
- [30] Mine A, Zhong Y, Liu J, Suzuki T, Najafzadeh S, Uchiyama T, Yin J X, Wu X, Shi X, Wang Z, Yao Y, and Okazaki K, *Direct observation of anisotropic Cooper pairing in kagome superconductor CsV_3Sb_5* <https://doi.org/10.48550/arXiv.2404.18472>.
- [31] Roppongi M, Ishihara K, Tanaka Y, Ogawa K, Okada K, Liu S, Mukasa K, Mizukami Y, Uwatoko Y, Grasset R, Konczykowski M, Ortiz B R, Wilson S D, Hashimoto K, Shibauchi T, *Bulk evidence of anisotropic s-wave pairing with no sign change in the kagome superconductor CsV_3Sb_5* 2023 Nat. Commu.14 667.
- [32] Wang Y, Kreisel A, Hirschfeld P J, and Mishra V, *Using controlled disorder to distinguish s_{\pm} and s_{++} gap structure in Fe-based superconductors* 2013 Phys. Rev. B 87 094504.
- [33] Mizukami Y, Konczykowski M, Kawamoto Y, Kurata S, Kasahara S, Hashimoto K, Mishra V, Kreisel A, Wang Y, Hirschfeld P J, Matsuda Y, and Shibauchi T, *Disorder-induced topological change of the superconducting gap structure in iron pnictides* 2014 Nat. Commun. 5 5657.
- [34] Mizukami Y, Konczykowski M, Matsuura K, Watashige T, Kasahara S, Matsuda Y, Shibauchi T, *Impact of Disorder on the Superconducting Phase Diagram in $BaFe_2(As_{1-x}P_x)_2$* 2017 J. Phys. Soc. Jpn. 86 083706.
- [35] Deutscher G, *Andreev-Saint-James reflections: A probe of cuprate superconductors* 2005 Rev. Mod. Phys. 77 109.
- [36] Daghero D and Gonnelli R S, *Probing multiband superconductivity by point-contact spectroscopy* 2010 Supercond. Sci. Technol. 23 043001.
- [37] Gonnelli R S, Daghero D, Ummerino G A, Stepanov V A, Jun J, Kazakov S M, and Karpinski J *Direct Evidence for Two-Band Superconductivity in MgB_2 Single Crystals from Directional Point-Contact Spectroscopy in Magnetic Fields* 2002 Phys. Rev. Lett. 89 247004.
- [38] Szabó P, Samuely P, Kačmarček J, Klein T, Marcus J, Fruchart D, Miraglia S, Marcenat C, and Jansen A G M, *Evidence for Two Superconducting Energy Gaps in MgB_2 by Point-Contact Spectroscopy* 2001 Phys. Rev. Lett. 87 137005.
- [39] Iavarone M, Karapetrov G, Koshelev A E, Kwok W K, Crabtree G W, Hinks D G, Kang W N, Choi E M, Kim H J, Kim H J, Lee S I, *Two-band superconductivity in MgB_2* 2002 Phys. Rev. Lett. 89 187002,
- [40] Feng X Y, Zhao Z, Luo J, Zhou Y Z, Yang J, Fang A F, Yang H T, Gao H J, Zhou R and Zheng Guo-qing, *Fully-gapped superconductivity with rotational symmetry breaking in pressurized kagome metal CsV_3Sb_5* 2025 Nat. Commun. 16 3643.